

Evidence of magnetization-dependent polaron distortion in $\text{La}_{1-x}\text{A}_x\text{MnO}_3$, $\text{A}=\text{Ca}, \text{Pb}$

C. H. Booth and F. Bridges

Department of Physics, University of California, Santa Cruz, California 95064

G. J. Snyder and T. H. Geballe

Department of Applied Physics, Stanford University, Stanford, California 94305

(Received 29 July 1996)

X-ray-absorption fine-structure measurements at the Mn K edge as a function of temperature were performed on $\text{La}_{1-x}\text{Ca}_x\text{MnO}_3$ and $\text{La}_{0.67}\text{Pb}_{0.33}\text{MnO}_3$. All samples have a metal-insulator (MI) transition near the ferromagnetic transition, except the $\text{Ca}_{0.5}$ sample, which does not have a MI transition. Near T_c for the samples exhibiting a MI transition, the Debye-Waller σ^2 for the Mn-O and Mn-Mn atom pairs increases rapidly with temperature. Since the change in σ^2 for the Ca/La atoms is much smaller, this nonthermal disorder must involve mainly the Mn and O atoms. These results strongly suggest that small polarons delocalize as the magnetization increases in materials which exhibit a MI transition. [S0163-1829(96)51646-2]

Although the basic physics behind the connection between the ferromagnetic (FM) transition, the conductivity, and the ‘‘colossal’’ magnetoresistance (CMR) in materials such as $\text{La}_{1-x}\text{A}_x\text{MnO}_3$ ($\text{A}=\text{one of certain divalent metals}$) is described by the double-exchange mechanism of Zener,¹ several features of the CMR materials are inconsistent with a model that only consists of double exchange.² Including spin-polarons and electron-electron interactions can help explain some features, such as the absolute value of T_c .³ Including thermal spin fluctuations may account for the conductivity.⁴ However, as pointed out by de Gennes,⁵ calculations of the conductivity may be inaccurate unless they include lattice interactions. One possibility is that the charge hopping in the double-exchange model induces structural-polaron formation.^{2,6} Such a formation would invalidate the assumption that the mean-free path is independent of the carrier mass, thereby enhancing the spin-spin coupling term in the double-exchange Hamiltonian.² If a polaron mechanism is to explain the discrepancies between the CMR effect with the double-exchange model, polarons must exist at least above T_c , and undergo a change in their dynamics below T_c with the result that the root-mean-square (rms) displacements of the atoms involved must be significantly reduced. Alternatively, if such changes are not observed, thermal spin fluctuations may be a better description.

Above T_c , the primary form of charge transport will be hopping, while below T_c the system will be in a metallic phase. In the former case, a moving charge may carry a lattice distortion along with it (small polaron), while in the latter case the lattice will not have time to react or have a small distortion on a larger scale (large polaron).

Nonstructural evidence for polaron formation above T_c is mounting.⁷⁻⁹ Recent results include: activated behavior in the resistivity⁷ and thermopower,⁸ and a large isotope shift of T_c with high O_{18} concentration.⁹

There are also a growing number of structural experiments that have shown evidence for polaron distortions in these materials.¹⁰⁻¹⁴ Neutron diffraction measurements on $\text{La}_{1-x}\text{Ca}_x\text{MnO}_3$ ($x=0.12, 0.21, \text{ and } 0.25$) have shown Jahn-Teller distortions of the O(2) (planar) atoms, producing three

Mn-O bond lengths in the planes separated by about 0.02 Å. Both the planar and axial (O(1)) oxygens have changes in the slope of the rms displacements with temperature at T_c in samples with metal-insulator (MI) transitions for the O(1), O(2), and La/Ca sites.¹⁰

A more compelling measurement should be provided by an experiment than can act as a *local* probe, since measurements of magnetization do not depend on long-range order. Such probes give information about the correlations between atomic positions.^{11,15} A pair distribution function analysis (PDF) of the same data as the diffraction analysis described above shows an increase of 0.12 Å in the distribution width of the Mn-O and O-O pairs.¹¹ Interestingly, the width in temperature of the transition is much broader in the PDF analysis, suggesting that the effect is present on a local scale far away from T_c . Another neutron diffraction study claims to see an anomalously long Mn-O peak at ~ 2.28 Å, which shows no temperature dependence, on a sample of $\text{La}_{0.67}\text{Sr}_{0.33}\text{MnO}_3$. Previous x-ray-absorption fine-structure (XAFS) measurements are qualitatively similar with these studies, measuring a change in the shape of the Mn-O distribution across T_c ,¹³ and a long Mn-O bond of ~ 2.5 Å.¹⁴

This work reports our XAFS results for the Mn-O atom pair. The data show that the smooth and rapid change in the Debye-Waller broadening parameter σ^2 near T_c for this bond as seen in PDF experiments¹¹ on $\text{A}=\text{Ca}_{0.21}$ and $\text{Ca}_{0.25}$, is present in our XAFS experiments on $\text{A}=\text{Ca}_{0.25}$, $\text{Ca}_{0.33}$, and $\text{Pb}_{0.33}$. This change is shown to be inconsistent with broadening due to thermal phonons. We also measure σ^2 for the next two near neighbors in the $\text{Ca}_{0.25}$ sample, and find the changes near T_c are smaller in the Mn-Ca/La scattering paths than in the Mn-O and the Mn-O-Mn paths, and therefore appear to mostly involve only the Mn and O atoms. Measurements of a sample which also has an antiferromagnetic transition but no metal-insulator transition ($\text{A}=\text{Ca}_{0.5}$) show no such effects, consistent with the insulating $\text{Ca}_{0.12}$ sample in the neutron scattering study.

Powder samples were made by the solid-state reaction of various proportions of the elemental oxides MnO, La_2O_3 , and PbO and the carbonate CaCO_3 . Further details can be

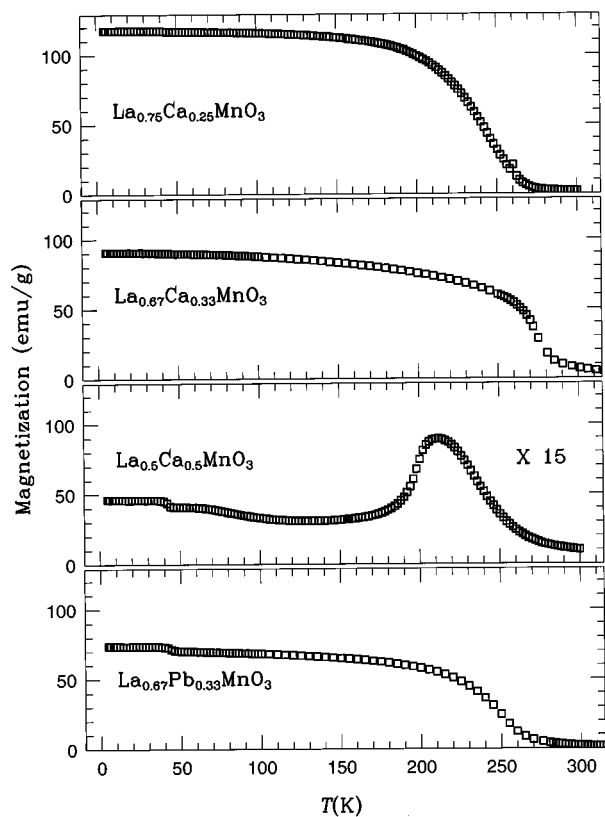


FIG. 1. Magnetization vs T for all samples. The applied fields were (from top to bottom) 2.5 kOe, 10 kOe, 2.5 kOe, and 5 kOe. The magnetization data for the $\text{Ca}_{0.50}$ data has been multiplied by 15.

found in Ref. 7. Magnetization vs T for the samples are shown in Fig. 1. T_c 's (estimated from 1/2 saturation magnetization) are 236 ± 5 K, 268 ± 5 K, and 241 ± 5 K for the $A = \text{Ca}_{0.25}$, $\text{Ca}_{0.33}$, and $\text{Pb}_{0.33}$ samples, respectively. The $\text{Ca}_{0.5}$ sample's T_c is 240 ± 10 K; it also has a Néel temperature around 210 K.

All absorption measurements were made in the transmission mode at the Stanford Synchrotron Radiation Laboratory on beamline (BL) 2-3 with Si(220) monochromator crystals and BL 10-2 with Si(111) crystals. Samples were ground, run through a $30 \mu\text{m}$ sieve and brushed onto scotch tape. Four layers of such tape were stacked to provide samples with a Mn K -edge step of roughly 0.3. Samples were then placed in an Oxford helium-flow cryostat. Temperature was monitored via a sensor on the probe about 2–6 cm from the sample. The temperature was regulated within 0.1 K, but the sample temperature could be as much as 2 K higher than the nominal temperature, especially for the higher temperatures.

Data were reduced following standard procedures.^{16–18} The XAFS were isolated by defining the parameter $\chi(k) = \mu(k)/\mu_0(k) - 1$, where k is the magnitude of the photoelectron wave vector, $\mu(k)$ is the total x-ray absorption due to the Mn K -shell excitation, and $\mu_0(k)$ is the part of $\mu(k)$ that does not include the interference of the outgoing part of the photoelectron wave function and the backscattered part. Although the monochromator crystals were more than 50% detuned, measurements of $\chi(k)$ from BL 2-3 were slightly lower in amplitude ($\sim 3\%$) than the measurements

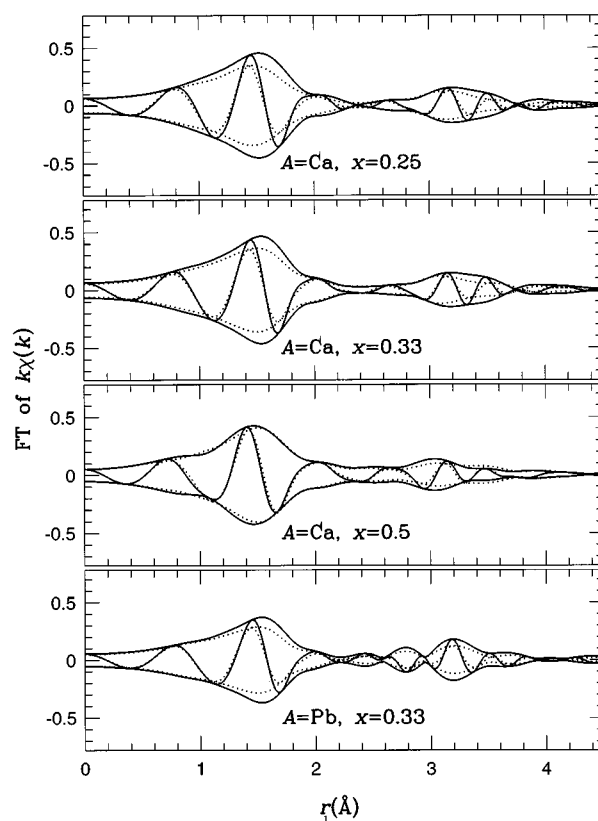


FIG. 2. r -space data of each sample at (solid) $T = 100$ K and (dotted) $T = 300$ K. Data are transformed from $3.5\text{--}14.5 \text{ \AA}^{-1}$ and Gaussian broadening by 0.3 \AA^{-1} .

from BL 10-2 at the same temperature, presumably from second-harmonic contamination. We therefore multiplied the data from BL 2-3 by 1.03 to allow better comparisons of the two data sets.

Fits to the data utilized theoretical standards as calculated by FEFF6.¹⁹ Theoretical standards (as opposed to standards obtained experimentally) allow for the measurement of an absolute broadening factor in the pair-distribution function, and thus allow for a direct comparison to diffraction results.

Figure 2 shows Fourier transforms (FT) of $k\chi(k)$ for each sample measured at 100 K and at 300 K. The first peak in these transforms is due to the Mn-O atom pair, while the broad peak centered near 3.2 \AA is really a multiplex with contributions from Mn-A, Mn-La, and the Mn-Mn pairs. The main feature to recognize in this figure is that the MI materials, all show a reduction in the Mn-O peak as T is raised from 100 K to 300 K. Such behavior may indicate a *soft* bond with a low Debye temperature, or possibly some other kind of change in the structural parameters. On the other hand, the Mn-O peak in the $\text{La}_{0.5}\text{Ca}_{0.5}\text{MnO}_3$ data is nearly unchanged (even near the FM transition), suggesting a relatively high Debye temperature and no other structural changes.

We fit each spectrum to standards of Mn-O, Mn-La, Mn-A, and the multiple scattering Mn-O-Mn path. These paths were calculated assuming the simple perovskite structure with no distortions. In particular, the Mn-O-Mn bond angle was taken to be 180° , even though for some compounds in the LaMnO_3 series, this angle can be as small as 160° . This

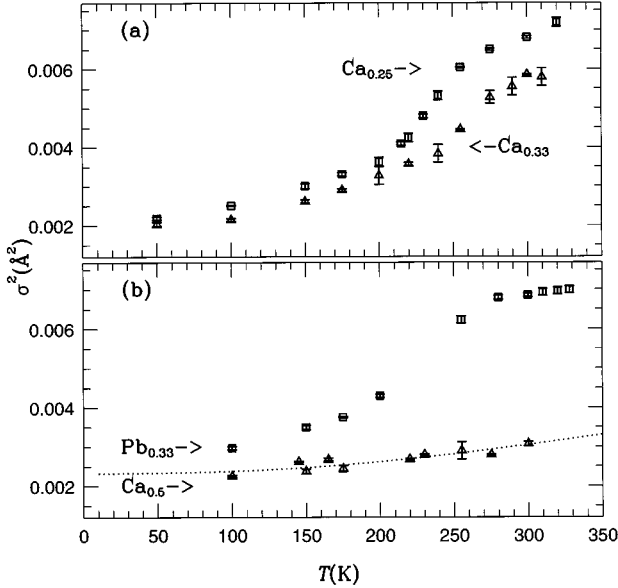


FIG. 3. σ^2 vs T for the Mn-O peak for all samples measured. The $\text{Ca}_{0.5}$ measurements are shifted down by 0.001 \AA^2 for clarity. Error bars indicate reproducibility of the data and fit, and in no way attempt to estimate systematic errors, which may be as large as 20%. The dotted line shows a correlated-Debye model for $\Theta_D = 950 \text{ K}$ with 0.0011 \AA^2 static broadening, also shifted down by 0.001 \AA^2 .

angle is expected to be close to 180° for these materials.²⁰ The amplitude reduction factor S_0^2 (an overall coefficient not accounted for by FEFF6) was based on the Mn-O peak for each sample and varied between 0.70 and 0.75, assuming 6 oxygens in the Mn-O peak. The Mn-O-Mn path was allowed to have its own S_0^2 of 0.55 to account for any possible change in the bond angle and for problems with FEFF6's multiple scattering calculations.

Fits to the Mn-O peak for the lowest temperature data are very similar for all samples. None of the bond lengths changed with temperature within the estimated error. The Mn-O bonds for the $A = \text{Ca}_{0.25}$, $\text{Ca}_{0.33}$, $\text{Ca}_{0.5}$, and $\text{Pb}_{0.33}$ are $1.95 \pm 0.005 \text{ \AA}$, $1.95 \pm 0.005 \text{ \AA}$, $1.92 \pm 0.005 \text{ \AA}$, and $1.96 \pm 0.005 \text{ \AA}$, respectively. These results are consistent with diffraction studies.^{10,20,21} Fits to the Mn-O broadening parameter for these data are presented in Fig. 3 and are consistent with the raw data in Fig. 2, as well as clearly showing a change in the local Mn-O environment. The σ^2 from the $\text{La}_{0.5}\text{Ca}_{0.5}\text{MnO}_3$ data is fit reasonably to a correlated-Debye model plus static disorder with $\Theta_D \cong 950 \text{ K}$. Interestingly, none of the data from the MI materials fits a Debye model very well in any temperature range. Each one starts out at the lowest temperatures with a σ^2 lower than the 50% Ca material (note that the $\text{Ca}_{0.5}$ results are shifted in Fig. 3), suggesting a higher Debye temperature or less static disorder. However, as T is increased (but still below the Curie point) σ^2 increases too sharply to be consistent with such a high Θ_D . A lower Θ_D would be possible except that an unphysically negative amount of static disorder would be necessary to describe the data. Within $\sim 40 \text{ K}$ of T_c , σ^2 begins to climb even more sharply, leveling off about 40 K above T_c . This behavior is fundamentally different from the behav-

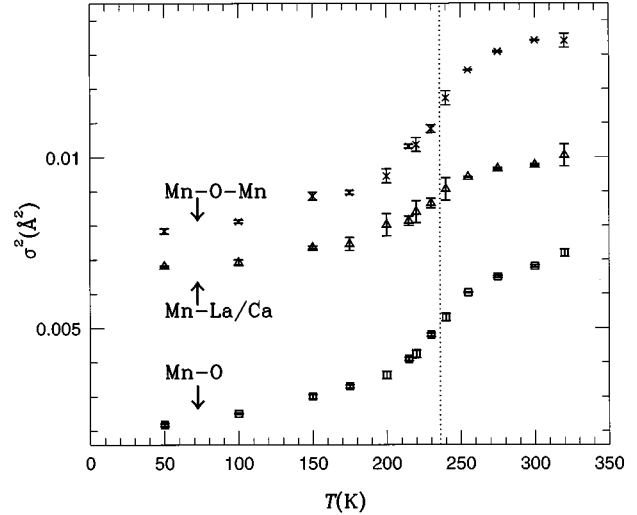


FIG. 4. σ^2 vs T for the $\text{La}_{0.75}\text{Ca}_{0.25}\text{MnO}_3$ Mn-O, Mn-La/Ca, and Mn-O-Mn scattering paths. The vertical dotted line marks T_c .

ior expected for phonon broadening with either a Debye or Einstein model, including static disorder. For these models, the tangent line to the data always has a positive intercept. A straight line though the data in the transition region has a negative intercept.

Fits to the further neighbor Mn-La, Mn-Ca, and Mn-O-Mn paths for the $\text{La}_{0.75}\text{Ca}_{0.25}\text{MnO}_3$ data are presented in Fig. 4. The relative intensity of the Mn-La and Mn-Ca signal could vary widely in the fits; interferences occur which make various combinations possible. Therefore, their intensities were held at a fixed 3:1 ratio, and their bond lengths were held equal in the fits. The Mn-Ca/La bond length was measured to be $3.38 \pm 0.02 \text{ \AA}$ and did not change with temperature. All bonds in Fig. 4 show similar increases of σ^2 near T_c . We obtain a rough measure of the size of the increase in σ^2 by extrapolating the low temperature fits to σ^2 past T_c and measuring the maximum difference between the data and this extrapolation. For the Mn-O bond in the 25% Ca sample, this increase is approximately 0.0022 \AA^2 , corresponding to an increase in σ of 0.047 \AA through T_c . (Note that σ 's add in quadrature.) If the disorder in the Mn-O pair is only along the a , b , and c axes, its projection onto the Mn-Ca/La pair is $\sim \Delta\sigma^2 \times (r_{\text{Mn-O}}/r_{\text{Mn-La/Ca}})^2 \sim 0.0022 \times (1.93/3.37)^2 = 0.0007 \text{ \AA}^2$ (ignoring any oxygen dimpling). The measured size of the anomaly for the Mn-La/Ca pair is, in fact, 0.0007 \AA^2 . This analysis suggests that either (a) only the Mn is distorting (unlikely, given that Mn is nearly 4 times heavier than oxygen, and there is no step in the Mn thermal parameters in Ref. 10), or (b) the Ca does distort, but only a fraction of the amount that the oxygens distort. In either case, we conclude that the distortion involves mostly the Mn and O atoms. This conclusion is supported by the 0.0028 \AA^2 jump for the Mn-O-Mn path. This path may have a larger step in σ^2 due to either a change in the correlation of the Mn positions or deviations of the bond angle from 180° ; these data cannot differentiate between these two possibilities. La-edge data should help further determine the nature of this disorder.

It is interesting to note the similarities between the magnetization data and the σ^2 fit results. Each distribution shows a long tail towards low temperature and approximately the same width in the transition region. Considering the magnetic data together with the high (~ 1000 K) Debye temperature necessary to describe the XAFS at the lowest temperatures, we are led to the conclusion that virtually *all* the temperature dependence demonstrated by the MI materials is magnetic in origin and caused by the degree of localization of polarons. At low temperatures and high magnetizations, the conduction electrons are allowed to hop freely between spin-aligned ions, and thus the polarons are effectively delocalized. Contrary to the usual thermal activation of polaron hopping, as T is increased towards T_c and the magnetization decreases, the polarons encounter more and more resistance in the form of unaligned ion spins and are thus more likely to become trapped, causing more localization and distortion. This trend will eventually reverse as T increases.⁷

Qualitatively, this distortion is consistent with Millis' prediction that the polaron distortion should cause an increase in the width of the distribution of the oxygen atoms near T_c of order 0.1 \AA .²

These data and this analysis are not consistent with a previous XAFS study.¹³ In that study, Tyson *et al.* measured a drastic change in the shape of the XAFS spectrum between $T=80$ K and 273 K, which they interpreted as a change in the Mn-O bond length distribution. As is clear from Fig. 2, we do not measure a fundamental difference between $T=100$ and 300 K (or anywhere in between), although there is an obvious difference in the amount of disorder. In another study, Tyson *et al.* measure a long Mn-O pair at $\sim 2.5 \text{ \AA}$,¹⁴

which is roughly in agreement with Louca *et al.*¹² We do see some evidence for such a peak; however there are several other interpretations, including an analysis artifact arising from FEFF6, and therefore do not include it in this analysis. Including this extra peak does not affect the results of this paper.

In conclusion, this work demonstrates a clear steplike increase in the width of the Mn-O bond near T_c for samples with a MI transition and a temperature dependence below T_c that is related to the magnetization of the sample. Since diffraction measurements do not show any step in the width parameters of any sites (they do show a change in slope at T_c),¹⁰ the steps we have measured in this work can be interpreted as arising from a more negatively correlated character in the positions of the atoms in the Mn-O and Mn-Mn pairs. In addition, we have shown that most of these displacements only involve the Mn and O atoms, as one expects from a polaron distortion. Lastly, we should point out that since diffraction measures essentially the same distortions above and below T_c , consistent with Jahn-Teller band splitting, the measurements reported in this work are separate and distinct from a change in the Jahn-Teller distortions.

We wish to thank G. Kwei for useful discussions and assistance in collecting the data. The experiments were performed at the Stanford Synchrotron Radiation Laboratory, which is operated by the U.S. Department of Energy, Division of Chemical Sciences, and by the NIH, Biomedical Resource Technology Program, Division of Research Resources. The experiment was partially carried out on UC/National Laboratories PRT beam time. The work was supported in part by NSF Grant No. DMR-92-05204.

-
- ¹C. Zener, Phys. Rev. **82**, 403 (1951).
²A. J. Millis, P. B. Littlewood, and B. L. Shraiman, Phys. Rev. Lett. **74**, 5144 (1995).
³C. M. Varma (unpublished).
⁴N. Furukawa, J. Phys. Soc. Jpn. **64**, 2734 (1995).
⁵P. G. de Gennes, Phys. Rev. **118**, 141 (1960).
⁶A. J. Millis, B. I. Shraiman, and R. Mueller, Phys. Rev. Lett. **77**, 175 (1996).
⁷G. J. Snyder *et al.*, Phys. Rev. B **53**, 14 434 (1996).
⁸M. Jaime *et al.*, Appl. Phys. Lett. **68**, 1576 (1996).
⁹G. Zhao, K. Conder, H. Keller, and K. A. Müller, Nature (London) **381**, 676 (1996).
¹⁰G. H. Kwei *et al.* (unpublished).
¹¹S. J. L. Billinge *et al.*, Phys. Rev. Lett. **77**, 715 (1996).
¹²D. Louca *et al.* (unpublished).
¹³T. A. Tyson *et al.*, Phys. Rev. B **53**, 13 985 (1996).
¹⁴T. A. Tyson *et al.*, Phys. Rev. B (to be published).
¹⁵C. H. Booth *et al.*, Phys. Rev. B **52**, R15 745 (1995).
¹⁶T. M. Hayes and J. B. Boyce, in *Solid State Physics*, edited by H. Ehrenreich, F. Seitz, and D. Turnbull (Academic, New York, 1982), Vol. 37, p. 173.
¹⁷G. G. Li, F. Bridges, and C. H. Booth, Phys. Rev. B **52**, 6332 (1995).
¹⁸F. Bridges, C. H. Booth, and G. G. Li, Physica B **208&209**, 121 (1995).
¹⁹S. I. Zabinsky, A. Ankudinov, J. J. Rehr, and R. C. Albers, Phys. Rev. B **52**, 2995 (1995).
²⁰R. Mahendiran *et al.*, Phys. Rev. B **53**, 3348 (1996).
²¹P. G. Radaelli *et al.*, Phys. Rev. Lett. **75**, 4488 (1995).